Dielectric charging phenomena in diamond films used in RF MEMS capacitive switches: The effect of film thickness

M. Koutsoureli, A. Zevgolatis, Samuel Saada, Christine Mer-Calfati, L. Michalas, G. Papaioannou, P. Bergonzo

Dielectric charging phenomena in diamond films used in RF MEMS capacitive switches: The effect of film thickness

M. Koutsoureli [a,□], A. Zevgolatis [a], S. Saada [b], C. Mer-Calfati [b], L. Michalas [a], G. Papaioannou [a], P. Bergonzo [b]

a Physics Department, University of Athens, 15784 Panepistimioupolis, Athens, Greece

b CEA, LIST, Diamond Sensors Lab., F-91191 Gif-sur-Yvette, France

* Corresponding author. E-mail address: mkoutsoureli@phys.uoa.gr (M. Koutsoureli)

Abstract

The present paper aims to provide a better insight to the dielectric charging phenomena of nano-crystalline diamond (NCD) films that are used in RF MEMS capacitive switches. The electrical properties of NCD films of various thicknesses are investigated with the aid of metal-insulator-metal (MIM) capacitors. The dominant conduction mechanisms have been identified by obtaining current-voltage characteristics in the temperature range from 300 K to 400 K and dielectric charging phenomena have been investigated by using thermally stimulated depolarization currents (TSDC) technique. The experimental results indicate a thermally activated conductivity for low electric field intensities while Hill-type conduction takes place for field intensities > 130 kV/cm. The conductivity as well as the defect density seems to increase with film thickness. Enhanced dielectric charging phenomena have been observed on thicker films and the injected charges are found to be trapped through the material's volume. These results indicate that thinner NCD films seem to be more promising for RF MEMS capacitive switches.

Keywords

RF MEMS switches, Reliability, Dielectric charging, Diamond, Electrical properties

1. Introduction

RF MEMS capacitive switches have received important research attention over the last years, since they offer several advantages over the conventional semiconductor counterparts, but they still suffer from reliability issues that hinder their commercialization [1]. Dielectric charging effect is one of the most important reliability problems of these switches, since it limits the device lifetime [1], [2].

In the dielectric films of MEMS capacitive switches charging takes place during the pull-in state, where charges are injected in the film from the metal electrodes under the presence of high electric fields (> 1 MV/cm). The discharge process takes place in the pull-up state of the switch, as the injected charges are collected from the bottom electrode plate. On the way to mitigate the dielectric charging phenomena several different approaches have been proposed, like the introduction of nanostructured dielectric films [3], that would exhibit appropriate dielectric permittivity and fast draining of the injected charges.

Diamond in micro-, nano- or ultra-nanocrystalline form has been used in MEMS capacitive switches and it has shown promising characteristics [4], [5], [6], [7], [8], [9], [10]. Diamond based RF MEMS exhibit satisfactory isolation [4], [5] and quite promising discharging behavior [5], [6], [8], [10]. The electrical characteristics of nanocrystalline diamond films for MEMS capacitive switches have been investigated [6], [9], [10] and the results have been applied in the modelling of the discharge process [10].

The conduction on poly/micro/nano/ultra-nanocrystalline diamond films takes place mainly through paths associated with the presence of extended defects at the grain boundaries [11]. On the other hand, lower conductivity is expected in the grain areas where the crystal quality is high and the defect density is smaller [12]. Non-diamond carbon, which is present at the grain boundaries area, forms sp^2 bonds while sp^3 bonds are formed in the crystalline diamond structures at the grain area [13]. More specifically it has been reported that the diamond film's electrical properties are directly related to the ratio of sp^2/sp^3 bonds [14], [15].

According to these, the grain size and the corresponding density of carbon sp^2 and sp^3 bonds are expected to determine the conductivity and therefore the electrical properties of nanocrystalline diamond (NCD) films. Regarding the material quality, it has been reported [14] that the increase of film thickness increases the crystalline quality of chemically vapor deposited (CVD) diamond films, since the growth process favors the increase of grain size and the decrease of grain boundary network [16]. However, Wiora et al. reported in [17] that there is a change of the nature of the grain boundaries, from graphitic in the case of larger grains to hydrogen terminated sp^3 carbon. The hydrogen content of NCD films has been found [17], [18] to increase with decreasing grain size whereas the sp^2 carbon content decreases. The conduction mechanisms in NCD films have been previously investigated [9], [10], [19], [20], [21], [22] though a correlation of conductivity parameters to the diamond film thickness has not been reported up to now, to the best of our knowledge.

In view of all these the present paper aims to provide a better insight to the effect of film thickness on the charge transport mechanisms, normal to film surface, that directly control the dielectric charging phenomena of NCD films when they are used in RF MEMS capacitive switches. The transport mechanisms of NCD films of various thicknesses have been investigated with the aid of Metal-Insulator-Metal (MIM) capacitors by monitoring current-voltage (I–V) characteristics at different temperatures and the thermally stimulated depolarization current (TSDC) technique has been applied in order to investigate the effect of film thickness to the dielectric charging phenomena.

2. Thermally stimulated depolarization currents (TSDC) method

Thermally stimulated depolarization currents (TSDC) technique is an efficient tool for investigating the relaxation phenomena of dipolar and space charge polarization [23]. In this assessment, a polarized sample is heated up to or above the polarization temperature (T_p) with a constant heating rate (β). When the half-life of this process becomes comparable to the time scale of the experiment (which is determined by the heating rate) discharge becomes measurable and it gives rise to a current measured in the external circuit [23]. A current peak is then obtained at a temperature where dipolar disorientation and/or carrier release from traps is activated. Taking into account that the total polarization usually arises from a combination of several individual effects with various relaxation times, a complete picture of the temperature dependent relaxation processes is thus obtained.

The time and temperature dependence of the dipolar polarization in dielectrics is determined by the competition between the orienting action of the polarization field and the randomizing action of thermal motions. Assuming an ideal rotational friction model (Debye) for establishing the polarization P, the decay of polarization of the dielectric material after the removal of the applied electric field is given by:

$$P(t) = P_S \; exp\left(-\frac{t}{\tau}\right) \qquad (1)$$

where P_S is the steady state polarization and τ is the dipolar relaxation time. The current density (J_{TSDC}) produced by the progressive decrease in polarization in the course of a TSDC experiment, where time and temperature vary simultaneously can be approximated [23] by:

$$J_{TSDC}(T) \approx \frac{P_S(T_p)}{\tau_0} . exp\left(-\frac{E_A}{k\,T}\right) . \exp\left[-\frac{1}{\beta\,\tau_0} . \frac{k\,T^2}{E_A} \exp\left(-\frac{E_A}{k\,T}\right)\right] \qquad (2)$$

where E_A is the depolarization mechanism's activation energy and τ_0 is the relaxation time at infinite temperature.

The stored charge (σ_{TSDC}) collected in the external circuit contributing to dielectric charging can then be calculated from the integration over the TSDC spectrum (from T_1 to T_2):

$$\sigma_{TSDC} = \frac{1}{\beta} . \int_{T_1}^{T_2} J_{TSDC}(T)\, dT \qquad (3)$$

3. Experimental details

In order to investigate the effect of film thickness on the conduction processes and on dielectric charging phenomena of nano-crystalline diamond (NCD) films, metal-insulator-metal (MIM) capacitors have been fabricated with 350 nm, 600 nm and 750 nm NCD films. The area of the utilized MIM capacitors was 450 × 450 μm^2.

The NCD films were deposited by microwave plasma assisted chemical vapor deposition (MPCVD) on a TiW/Au/Si substrate. Plasma treatments were performed in a home-made designed MPCVD reactor equipped with a 2.45 GHz–2 kW SAIREM microwave generator. The base pressure inside the chamber was about 10^{-9} mbar. A nanoseeding technique has been used to achieve a high nucleation density at the early stage of diamond growth in order to form a continuous diamond film. The nanoseeding technique that has been applied consists of the deposition of diamond nanocrystals dispersed in polyvinyl alcohol (PVA) on a substrate surface by spin coating [24]. Then, the synthesis of the NCD films was performed by MPCVD using a mixture of 0.6% methane (CH_4) diluted in hydrogen (H_2). The total pressure and the microwave power during the growth were maintained at 35 mbar and 900 W, respectively. This induced a substrate temperature of 1023 K. During growth the film thickness was monitored by a home-made laser interferometry system [25], which was used to stop the experiment at the desired thickness. We mention that all thickness measurements have been performed with the aid of spectroscopic ellipsometry using a bilayer model in order to take into account the roughness of the film and the measurement error can be estimated < 5%. The deposited NCD films have a columnar structure (Fig. 1a) and SEM images indicate that the grain size is increased with film thickness (Fig. 1b).

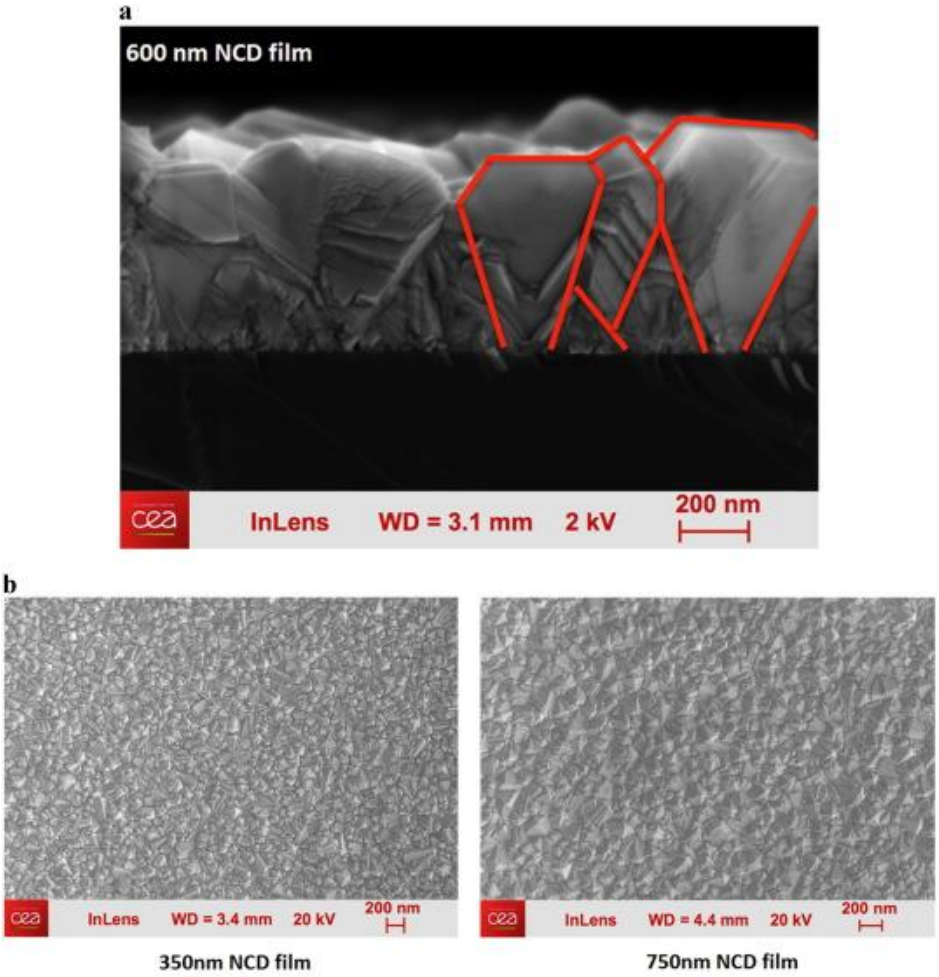

Fig. 1.
a: SEM image of 600 nm NCD films (cross section) indicating the structure of selective columnar growth.

b: SEM images of 350 nm and 750 nm NCD films (top view) used in utilized MIM capacitors.

The dominant conduction mechanisms of NCD films have been investigated by obtaining the current-voltage (I–V) characteristics in a vacuum cryostat (pressure ~ 10^{-3} Torr). Acquisition was performed with the aid of Keithley 6487 voltage source/picoampere meter, controlled via LabView in order to include an appropriately time delay between the application of each bias step and the corresponding current measurement and to overcome any transient effects ensuring steady state condition measurements (leakage current), in the temperature range from 300 K to 400 K and for field intensities up to 200 kV/cm. Apart from these, thermally stimulated depolarization currents (TSDC) technique has been applied to our samples in order to investigate dielectric charging phenomena. The TSDC current of each sample was measured with the aid of a Keithley 6487 voltage source/picoampere meter in the temperature range of 200 K–450 K and a heating rate of 2.5 K/min. Finally, the polarization field intensity was 100 kV/cm and the polarization temperature was 450 K.

4. Results and discussion

In order to investigate the effect of film thickness on the conduction processes of NCD films we have obtained I–V characteristics for temperatures up to 400 K.

The conductivity σ = J/F is found to increase with film thickness (Fig. 2) and for field intensity levels lower than 130 kV/cm it has been found to be thermally activated, with an activation energy (0.6 eV–0.8 eV) that decreases as the film thickness increases (Fig. 2). This process, for low electric field intensities, has been generally attributed to either hopping below room temperature [9], [21] or band conduction mechanisms at higher temperatures [21].

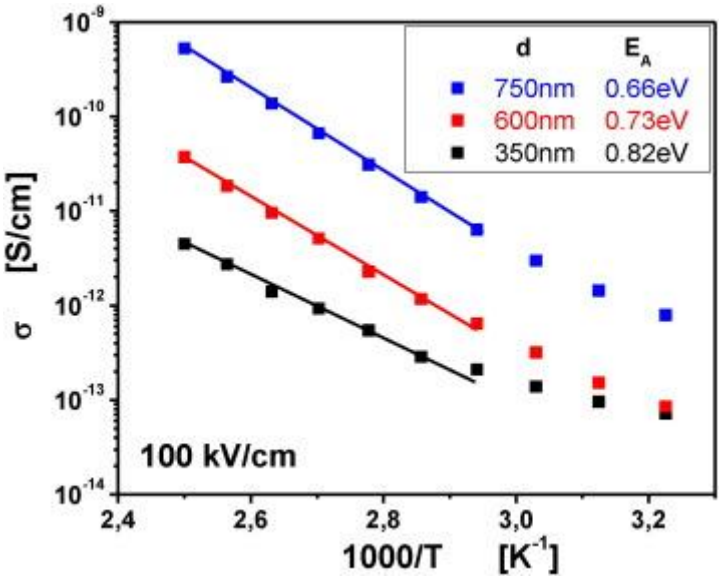

Fig. 2. Arrhenius plot of conductivity plotted for all samples when the applied electric field is 100 kV/cm. The activation energy of each sample is also presented.

For field intensities larger than 130 kV/cm and for temperatures larger than 320 K the experimental results indicate (Fig. 3) that the conductivity of all samples obeys the Frenkel-Poole conduction as modified by Hill when a sufficient overlapping of Coulomb potential occurs [19], [20], [26]. This conduction mechanism involves discrete levels (at E_i from the conduction band) whose overlap of the Coulombic potentials is sufficient to allow the hopping of carriers from site to site. According to Hill-type conduction [26] the current density (J) at a given temperature (T) obeys by the following relationship:

$$J = 2eNs\,(kT)^2 v exp\left(-\frac{E_p}{kT}\right)\, sinh\left(\frac{eFs}{2kT}\right) \qquad (4)$$

where k is the Boltzmann's constant, e is the electron charge, N is the density of the centers, s is the distance separating two centers, v is the attempt to escape frequency and $\beta = e^{3/2}(\pi\varepsilon\varepsilon_0)^{-1/2}$ is the Frenkel-Poole constant for the material (ε is the relative permittivity of the material and ε_0 is the

vacuum permittivity). Finally, E_p is the potential barrier over which the carriers hop from one center to another and it is given by:

$$E_p = E_i - \frac{\beta^2}{e.s} \qquad (5)$$

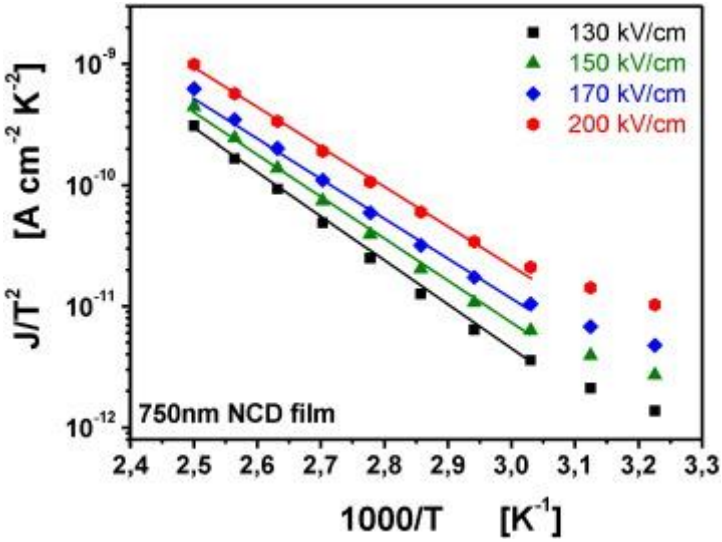

Fig. 3. Signature plot of Hill conduction for 750 nm NCD films, in agreement to Eq. (6) for different electric field intensities.

From Eq. (4) and taking into account that $sinh\left(\frac{eFs}{2\,kT}\right)$ at high fields [20] we obtain that:

$$\frac{J}{T^2} \propto exp\left(-\frac{E_A}{kT}\right) \qquad (6)$$

where the activation energy E_A is related to the electric field as:

$E_A = E_P - \frac{e.s.F}{2}$. Thus, from the linear variation of E_A with F and from Eq. (5) we have deduced the values of s and E_i for each sample (Table 1).

NCD film thickness	**Field < 130 kV/cm Thermal activation**	**Field > 130 kV/cm Hill conduction**		**TSDC**	
	E_A [eV]	**s [nm]**	**N [cm^{-3}]**	**E_i [eV]**	**σ_{TSDC} [C/cm^2]**
350 nm	0.66 ± 0.02	52.3 ± 2.6	(7.0 ± 1.0) × 10^{15}	0.84 ± 0.02	(4.71 ± 0.07) × 10^{-6}
600 nm	0.73 ± 0.02	33.6 ± 0.3	(2.6 ± 0.1) × 10^{16}	0.91 ± 0.01	(5.43 ± 0.04) × 10^{-6}
750 nm	0.82 ± 0.01	28.8 ± 0.5	(4.2 ± 0.2) × 10^{16}	0.95 ± 0.01	(7.94 ± 0.06) × 10^{-6}

Table 1. Electrical characteristics of NCD films obtained from our experimental data. The errors of our calculations are also shown.

Here it must be emphasized that the defect levels in polycrystalline diamond films have been intensively investigated [21], [22], [27], [28], [29], [30], since transport processes are strongly affected by trapping and detrapping at these levels. Deep defect levels with activation energy of 1 eV [22], [28], [29] or 1.5 eV [27], [30] as well as swallower ones with activation energy of 0.3 eV [21], [27], [29] and 0.7 eV [21], [27], [28] have been reported on chemically vapor deposited (CVD) diamond films and attributed mainly to the presence of non-diamond carbon material at grain boundaries [21], [22]. It has been also reported [31] that the e-beam evaporation as a contact deposition technique has a strong influence on deep trap filling by free carriers, which results to an increase of carrier drift length before trapping. However, carrier release from these traps starts at temperatures higher than 200 °C as reported by Hordequin et.al. [31]. In addition, we mention that on RF MEMS switch applications in

harsh environment (e.g. over the military) the temperature ranges from − 55 to 125 °C [32] and at higher temperatures suitable for bonding (300–400 °C) the membrane (or cantilever) may be displaced by ± 1–5 μm thus making the switch unusable [33]. Taking these into consideration, we are led to the conclusion that the deep traps of NCD films will be filled as soon as the switch will be actuated and the discharge process will take place with the deep traps filled. Thus, the device performance will be mainly affected by the charge trapping and emission from the shallower traps and therefore the assessment methods used in the present work do not investigate the trapping and detrapping processes on deep traps of NCD films.

The obtained energy levels E_i can be then directly correlated to conduction paths at grain boundaries, that correspond to activation energy levels in the range of 0.7–1 eV [21], [22], [27], [28]. The increase of NCD film thickness has been found to result in an increase of the energy level E_i (Fig. 4) while the mean separation distance (s) between two centers slightly decreases (Table 1). Moreover, assuming that the density N of the centers responsible for the conduction is $N \approx \frac{1}{s^3}$ [19] we obtain that the density N increases with film thickness (Table 1).

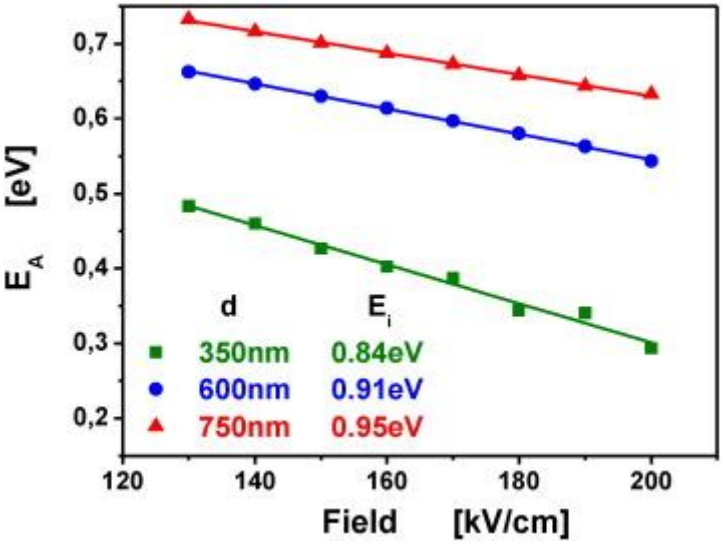

Fig. 4. The linear decrease of activation energy E_A with field intensity for the utilized NCD films. The energy level E_i increases with film thickness.

It is important to mention that band conduction at low fields as well as Hill conduction at higher fields has been previously reported in the literature [9], [10], [19], [20] on diamond films and the obtained values for energy levels E_i, for the mean separation distance s and the defect density N are in agreement to previously reported values on diamond films [9], [10], [19], [20].

As already mentioned, the growth process favors the decrease of grain boundary network [16], which implies that the film conductivity as well as the defect density should decrease as the film thickness increases, on the contrary to our results. However, it is possible that there is a change of the nature of the grain boundaries, from graphitic in the case of larger grains to hydrogen terminated sp^3 carbon, as previously reported by Wiora et al. [17]. Moreover, it has been found [17], [18] that the decrease of grain size may also cause an increase of hydrogen content in diamond films and the incorporated hydrogen atoms are most likely bonded within the grain boundary region [18]. Taking these into account, in the utilized NCD films the decrease of film thickness results to a decrease of grain size and a possible change in the nature of grain boundaries (e.g. a decrease of the sp^2 carbon content due to increased hydrogen content) may be responsible for the decrease of defect density and conductivity that has been observed. In addition, the fact that the mean hopping distance (in Hill conduction mechanism) has been found to decrease as the film thickness increases comes along with the result that defect density is found to be larger on thicker films.

Finally, dielectric charging phenomena have been investigated with the aid of TSDC method. The resulting TSDC spectra have an envelope that exhibits Arrhenius-like behavior (Fig. 5) with an

activation energy of about 0.8–0.9 eV in all samples. These energy levels are in good agreement with previously reported trap levels in diamond films [21], [22], [27], [28], [29], [30].

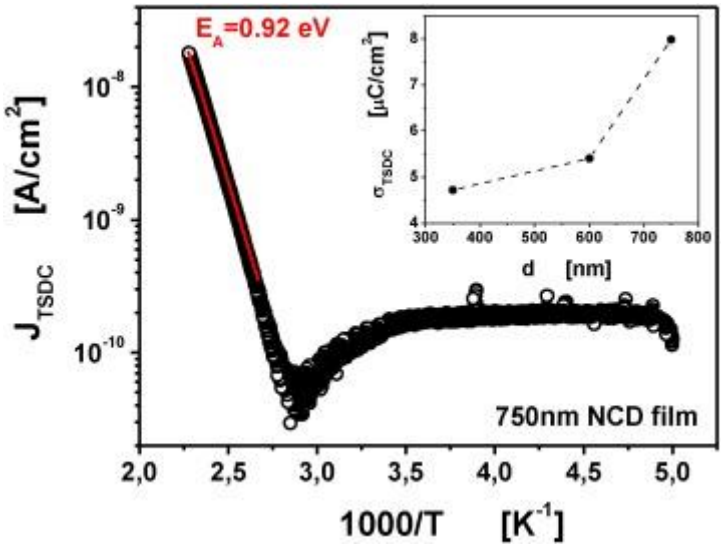

Fig. 5. Arrhenius plot of TSDC spectrum for 750 nm NCD films. The inset graph shows the increase of total charge density measured in the external circuit during TSDC with film thickness.

Moreover, it is found that dielectric charging is enhanced as the thickness of NCD films increases (inset of Fig. 5 and Table 1), since the total charge density σ_{TSDC} measured in the external circuit during TSDC has been found to be larger on thicker NCD films. The latter indicates that the injected charges are trapped through material's volume and not at the surface of the films, near the metal contacts.

5. Conclusions

The conduction processes of NCD films that can be used in RF MEMS switches and the effect of film thickness on the material's electrical properties have been investigated in this paper.

The dominant conduction mechanisms have been identified by obtaining current-voltage characteristics in the temperature range from 300 K to 400 K and dielectric charging phenomena have been investigated by using thermally stimulated depolarization currents (TSDC) technique. The films' conductivity has been found to be thermally activated for low electric field intensities while Frenkel-Poole conduction modified by Hill dominates the conduction process when the electric field becomes stronger than 130 kV/cm. The increase of film thickness results to an increase of conductivity, an increase of defect density while the energy levels of the traps associated to Hill conduction mechanism shift a little deeper in the energy gap of the material. These results have been attributed to a possible change on the nature of grain boundaries as the grain size increases, from graphitic in the case of larger grains to hydrogen terminated sp^3 carbon. Finally, TSDC assessment revealed that the injected charges are trapped through material's volume, thus dielectric charging is enhanced as the NCD film thickness increases.

Taking into account that in order to increase the reliability of a capacitive RF MEMS switch it is important to eliminate dielectric charging effects, the above mentioned conclusions indicate that thinner NCD films seems to be more promising for these devices. We also mention that the use of thinner NCD films will also improve the switch RF performance, since it will cause an increase of the down-state capacitance which results to higher isolation.

Acknowledgement

The first author, Matroni Koutsoureli, would like to thank “IKY Fellowships of Excellence for Postgraduate Studies in Greece – Siemens Program” that takes place in the framework of the Hellenic Republic – Siemens Settlement Agreement. The other authors acknowledge the support from the FP7

ENIAC/ESPA-GR project “Microsystem Based on Wide Band Gap Materials Miniaturized and Nanostructured RF-MEMS” NANOCOM under GA: 270701-2, ENIAC call 3.

References

[1] G.M. Rebeiz. RF MEMS Theory, Design and Technology. Hoboken, Wiley, New Jersey, USA (2003), pp. 185-215

[2] W.M. Van Spengen. J. Micromech. Microeng., 22 (2012), p. 074001.

[3] G. Papaioannou, L. Michalas, M. Koutsoureli, S. Bansropun, A. Gantis, A. Ziaei. Proc. IEEE 14th Top. Meet. on Silicon Monolithic Int. Circ. in RF Syst. (SiRF) (2014), pp. 98-100

[4] J. Chee, R. Karru, T.S. Fisher, D. Peroulis. Proc. 35th Europ. Microw. Conf. (2005), pp. 581-584

[5] S. Balachandran, D. Hoff, A. Kumar, T. Weller. Proc. IEEE MTT-S Int. Microw. Symp. Dig. (2009), pp. 1657-1660

[6] C. Goldsmith, A. Sumant, O. Auciello, J. Carlisle, J.C.M. Hwang, C. Palego, W. Wang, R. Carpick, V.P. Adiga, A. Datta, C. Gudeman, S. O'Brien, S. Sampath. Proc. IEEE Int. Microw. Symp. Dig. (2010), pp. 1246-1249

[7] C. Chen, Y. Tzeng, E. Kohn, C.H. Wang, J.K. Mao.vDiam. Relat. Mater., 20 (2011), pp. 546-550

[8] L. Michalas, S. Saada, M. Koutsoureli, C. Mer, A. Leuliet, P. Martins, S. Bansropun, G. Papaioannou, P. Bergonzo, A. Ziaei. Proc. of 43rd Europ. Microw. Conf., EuMA (2013), pp. 1335-1338

[9] L. Michalas, *et al.* Proc. IEEE Int. Reliab. Phys. Symp. (IRPS), 6B (2013), pp. 3.1-3.7

[10] L. Michalas, M. Koutsoureli, S. Saada, C. Mer-Calfati, A. Leuliet, P. Martins, S. Bansropun, G. Papaioannou, P. Bergonzo, A. Ziaei. J. Micromech. Microeng., 24 (2014), p. 115017

[11] T. Sugino, Y. Muto, J. Shirafuji, K. Kobashi. Diam. Relat. Mater., 2 (1993), pp. 797-802

[12] G. De Cesare, S. Salvatori, R. Vincenzoni, P. Ascarelli, E. Cappelli, F. Pinzari, F. Galluzzi. Diam. Relat. Mater., 4 (1995), pp. 628-631

[13] K. Kobashi, K. Nishimura, Y. Kawate, T. Horiuchi. Phys. Rev. B, 38 (1988), pp. 4067-4084

[14] C. Jany, A. Tardieu, A. Gicquel, P. Bergonzo, F. Foulon. Diam. Relat. Mater., 9 (2000), pp. 1086-1090

[15] E.J. Correa, Y. Wu, J.-G. Wen, R. Chandrasekharan, M.A. Shannon. J. Appl. Phys., 102 (2007), p. 113706

[16] M.A. Plano, S. Zhao, C.F. Gardinier, M.I. Landstrass, D.R. Kania, H. Kagan, K.K. Gan, R. Kass, L.S. Pan, S. Han, S. Schnetzer, R. Stone. Appl. Phys. Lett., 64 (1994), pp. 193-195

[17] M. Wiora, K. Bruhne, A. Floter, P. Gluche, T.M. Willey, S.O. Kucheyev, A.W. Van Buuren, A.V. Hamza, J. Biener, H.J. Flecht. Diam. Relat. Mater., 18 (2009), pp. 927-930

[18] S. Michaelson, O. Ternyak, R. Akhvlediani, A. Hoffman, A. Lafosse, R. Azria, O.A. Williams, D.M. Gruen. J. Appl. Phys., 102 (2007), p. 113516

[19] P. Gonon, A. Deneuville, F. Fontaine, E. Gheeraert. J. Appl. Phys., 78 (1995), p. 6633

[20] P. Gonon, Y. Boiko, S. Prawer, D. Jamieson. J. Appl. Phys., 79 (1996), p. 3778

[21] E.P. Visser, G.J. Bauhuis, G. Janssen, W. Vollenberg, W.J.P. van Enckevort, L.J. Giling. J. Phys. Condens. Matter, 4 (1992), pp. 7365-7376

[22] Y. Muto, T. Sugino, J. Shirafuji, K. Kobashi. Appl. Phys. Lett., 59 (1991), pp. 843-845

[23] J. Vandershueren, J. Casiot. P. Braunlich (Ed.), Topics in Applied Physics: Thermally Stimulated Relaxation in Solids, vol. 37, Springer-Verlag, Berlin, Germany (1979)

[24] E. Scorsone, S. Saada, J.C. Arnault, P. Bergonzo. J. Appl. Phys., 106 (2009), p. 014908

[25] S. Saada, S. Pochet, L. Rocha, J.C. Arnault, P. Bergonzo. Diam. Relat. Mater., 18 (2009), pp. 707-712

[26] R.M. Hill. Philos. Mag., 23 (1971), pp. 59-86

[27] D. Tromson, P. Bergonzo, A. Brambilla, C. Mer, F. Foulon, V.N. Amosov. Phys. Stat. Sol. A, 174 (1999), pp. 155-164

[28] D. Tromson, P. Bergonzo, A. Brambilla, C. Mer, F. Foulon, V.N. Amosov. J. Appl. Phys., 87 (2000), pp. 3360-3364

[29] M. Bruzzi, D. Menichelli, S. Sciortino, L. Lombardi. J. Appl. Phys., 91 (2002), pp. 5765-5774

[30] J. Alvarez, J.P. Kleider, P. Bergonzo, D. Tromson, E. Snidero, C. Mer. Diam. Relat. Mater., 12 (2003), pp. 546-549

[31] C. Hordequin, D. Tromson, A. Brambilla, P. Bergonzo, F. Foulon. J. Appl. Phys., 90 (2001), pp. 2533-2537

[32] Y. Xiaobin, Z. Peng, J.C.M. Hwang, D. Forehand, C.L. Goldsmith. IEEE Trans. Device Mat. Reliab., 6 (2006), pp. 556-563

[33] G.M. Rebeiz, J.B. Muldavin. IEEE Microw. Mag., 2 (2001), pp. 59-71